Available online at www.sciencedirect.com
ScienceDirect
Journal of Catalysis 254 (2008) 304–309
JOURNAL OF CATALYSIS
www.elsevier.com/locate/jcat

What determines the catalyst's selectivity in the ethylene epoxidation reaction

Anton Kokalj [a,b,*], Paola Gava [b], Stefano de Gironcoli [b], Stefano Baroni [b]

[a] *Jožef Stefan Institute, Jamova 39, SI-1000 Ljubljana, Slovenia*
[b] *INFM-CNR DEMOCRITOS Theory@Elettra group and SISSA, Via Beirut 2-4, 34014 Trieste, Italy*

Received 25 September 2007; revised 31 December 2007; accepted 3 January 2008

Available online 7 February 2008

Abstract

The selectivity of a catalyst in ethylene epoxidation reaction was addressed using quantum mechanical computer simulations. We found that the catalyst's selectivity in the reaction of oxametallacycle to form ethylene epoxide (EO) rather than the competing acetaldehyde (Ac) is determined in part by the differential bonding affinity of the catalyst toward the O and C atoms of the oxametallacycle. This interplay between O– and C–metal bond strength is due to the different structures of the two transition states. Based on this finding, we introduce a new indicator that determines the difference between the EO and Ac activation energies in the oxametallacycle reaction remarkably well for a number of different materials.

Keywords: Ethylene epoxidation; C–H activation; Density functional calculations; Heterogeneous catalysis; Reaction mechanisms

1. Introduction

The ethylene epoxidation is one of the most important selective oxidation processes occurring on metal catalysts [1–4]. Silver is a remarkably good catalyst for this reaction, with a selectivity of up to 80% at high temperature and high pressure in the presence of promoters such as Cl and Cs [1–3]. It has been established [5–12] that the ethylene epoxidation proceeds through an oxametallacycle (OMC) intermediate[1] [13–15], which then transforms to either ethylene epoxide (EO) or acetaldehyde (Ac), with the latter reaction leading to undesired total combustion. Despite the many computational studies [16–22] spurred by this finding, where the reaction mechanism of OMC conversion to EO and Ac have been characterized, knowledge of the specific surface factors that lead to different competing reaction products remains elusive. Consequently, we explored the catalyst's activity and selectivity using quantum mechanical computer simulations, based on density functional theory (DFT) and the plane-wave pseudopotential scheme. We first demonstrated that for ethylene epoxidation to occur, the catalyst must be mild enough as to form and to stabilize an OMC, rather than break C–H bonds, either in the reactant (ethylene) or in the intermediate state (OMC). We then found that for OMC to transform to EO rather than to Ac, its C–metal bond must be sufficiently weak with respect to the O–metal bond, and the adsorbed EO should be stabilized against the adsorbed Ac. Finally, we propose a simple indicator for catalyst selectivity that improves considerably on the straight application of the Brønsted–Evans–Polanyi (BEP) relation to both the EO and Ac formation reactions. Our model, which is suggested by the inspection of the two transition states from the OMC, explains why Cu/Ag alloys displays a better selectivity than pure silver for the formation of EO, as has been suggested recently [17].

Although there is growing evidence that ultrathin oxide overlayers [23–25], may play an important role in the reactivity of metal catalysts under ordinary industrial conditions, we focus

* Corresponding author at: Jožef Stefan Institute, Jamova 39, SI-1000 Ljubljana, Slovenia. Fax: +386 1 477 38 22.
E-mail address: Tone.Kokalj@ijs.si (A. Kokalj).
URL: http://www-k3.ijs.si/kokalj/.

[1] In the OMC intermediate, one of the two C atoms of ethylene binds to the metal substrate through an oxygen bridge, and the other binds directly to one or more metal atoms.

0021-9517/$ – see front matter
doi:10.1016/j.jcat.2008.01.008

here on model catalysts, which allows us to gain insight into the fundamental factors that govern the selectivity at atomic scale, with a reasonable computational effort. In particular, we consider the (100) and (111) surfaces of IB metals, as well as of a more reactive catalyst, such as rhodium. We consider and compare several competing reaction mechanisms.

2. Computational details

The reactions are modeled on (100) and (111) surfaces by (2×2), (3×2), and (4×3) supercells of periodically repeated slabs. Reaction pathways are determined as the minimum energy paths (MEPs) connecting the reactants (initial state: IS) with the products (final state: FS), using the climbing-image nudged elastic band method [26]. The configuration of maximum energy along the MEP is identified as the transition state (TS), the energy difference of which with respect to the IS gives the activation energy, E^*. Calculations were performed using the PBE density functional [27] as implemented in the `PWscf` code [28] of the `Quantum ESPRESSO` distribution [29]. Kohn–Sham orbitals were expanded in a plane-wave basis set to a kinetic energy cutoff of 27 Ry (216 Ry for the charge-density cutoff), whereas core electrons were treated by ultra-soft pseudopotentials [30,31]. For the (2×2), (2×3), and (4×3) supercells, the Brillouin zone integrations were performed with (4×4), (4×3), and (2×3) uniform shifted k-mesh, respectively. Molecular graphics were produced by the `XCRYSDEN` graphical package [32]. Further computational details are provided in the Supplementary material.

3. Results and discussion

Table 1 presents the activation energies calculated for a number of relevant reactions on Rh(100) and Ag(100): (1) OMC formation; (2) C–H bond-breaking (for OMC the H cleavage from the C atom bonded to metal is considered); (3) C–C bond breaking; (4) product formation from the OMC intermediate; and (5) ethylene formation back from OMC, which can be seen as C–O bond-breaking. It is known from experiments that more reactive metals break the C–H bond (and thus burn the ethylene), whereas Ag does not [1]. It has been suggested that on Ag, C–H bonds may be activated by chemisorbed oxygen [1,2,33]. The results in Table 1 support these conclusions: on the more reactive Rh surface, ethylene dehydrogenation (2.1) and OMC formation (1) followed by its dehydrogenation (2.3) are by far the most favorable reactions, whereas the formation of EO and Ac, (4.1) and (4.2), are the least probable. Our results are in agreement with experimental results [34,35] that indicate rapid decomposition of OMC on Rh. Among the two suggested decomposition paths, C–C and C–H bond cleavage, our calculations strongly favor the latter. On Ag, the most favorable reactions are instead the formation of OMC, (1), and its reverse, (5), followed by the transformation of OMC to EO and Ac, (4.1) and (4.2). Dehydrogenation reactions are less probable; in particular, C–H bond activations by the metal itself, (2.1) and (2.3), have higher barriers than reaction (2.2), where C–H bond-breaking is facilitated by chemisorbed oxygen. These results clearly show that a mild catalyst is required for the formation of EO and/or Ac; otherwise, other competing reactions, particularly those involving C–H bond-breaking, would occur. Still, the catalyst should be sufficiently reactive to form an ethylene OMC. Silver, as well as other noble IB metals [20,21,36–38], fulfill these requirements.

Table 1
Activation energies (E^*) of some representative reactions that ethylene and its oxametallacycle (OMC) may undergo on oxygen-covered Rh(100) and Ag(100) surfaces. Energies quoted as lower bounds are estimated from the energy difference between the products and the reactants. As for the OMC dehydrogenation, reaction 2.3, the C–H bond cleavage of the C atom bonded to the metal is considered

#	Reaction	E^* (eV)	
		Rh(100)	Ag(100)
1	$C_2H_4(g) + O(a) \rightarrow OMC(a)$	0.31	0.33
2.1	$C_2H_4(a) \rightarrow C_2H_3(a) + H(a)$	0.46	>1.41
2.2	$C_2H_4(a) + O(a) \rightarrow C_2H_3(a) + OH(a)$	1.45	1.03
2.3	$OMC(a) \rightarrow C_2H_3O(a) + H(a)$	0.26	>1.55
3.1	$C_2H_4(a) \rightarrow 2CH_2(a)$	1.33	>3.08
3.2	$OMC(a) \rightarrow CH_2(a) + CH_2O(a)$	1.62	>1.69
4.1	$OMC(a) \rightarrow Ac$	1.90	0.83
4.2	$OMC(a) \rightarrow EO$	2.17	0.87
5	$OMC(a) \rightarrow C_2H_4 + O(a)$	1.13	0.68

Fig. 1 displays reaction profiles for the formation of EO and Ac starting from gas-phase ethylene and oxygen-covered Cu(100), Ag(100), and Au(100).[2] The barrier for the formation of OMC is greatest on Cu(100) and almost vanishes on Au(100). However, in the reverse direction, the barrier for the formation of the OMC starting from EO is the smallest on Cu, indicating that it should be possible to isolate OMC on Cu, as has been done on Ag [8,10]. As for the formation of EO and Ac from the OMC intermediate, our results show a similar trend as found in a previous study of IB-metal (111) surfaces [20,21]. Ag displays the smallest barriers for the formation of both EO and Ac; the largest barriers occur on Cu, but Cu is intrinsically more selective than Ag for the formation of EO [20]: the activation energy for the formation of EO is smaller than that for Ac, whereas the opposite is true for Ag and Au, with the latter being the least selective for the formation of EO. However, on Cu, the formation of EO is endothermic from either OMC or gas-phase ethylene (the opposite is true on Ag, see Fig. 1), and Torres et al. anticipated that short contact times might be required to limit the decomposition of the EO product [20]. It also has been reported that an oxide film forms on Cu surfaces that is catalytically inert toward EO formation [40,41]. Another problem with Cu is that it is sufficiently reactive for the C–H bond to break significantly, at least on more open surfaces or near surface defects. On Cu(100) the calculated activation energy for OMC dehydrogenation, reaction (2.3), is indeed 1.31 eV, lower than for the formation of EO and Ac (1.49 and 1.61 eV, respectively). On the more compact (111) surface, this problem would be substantially alleviated. Namely, the latter two relevant activation energies are smaller, 1.27 and 1.44 eV, respectively,

[2] Au(100) actually undergoes a hexagonal reconstruction. See Ref. [39], and references therein. For the sake of establishing chemical trends, such a reconstruction was not considered in our simulations.

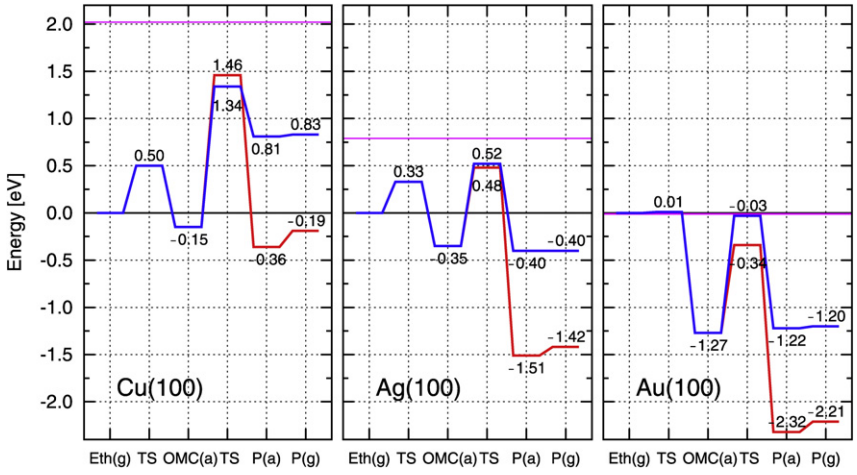

Fig. 1. Reaction profiles for the formation of ethylene epoxide (EO, blue line) and acetaldehyde (Ac, red line) starting from the gas-phase ethylene and chemisorbed atomic oxygen on Cu(100)-(2 × 2), Ag(100)-(2 × 2), and Au(100)-(2 × 2). The zero level is the energy of gas-phase ethylene and chemisorbed atomic oxygen, whereas the energy position of the gas-phase $\frac{1}{2}O_2$ is marked by violet horizontal line. The labels on the abscissa have the following meaning: Eth—ethylene, TS—transition-state, OMC—oxametallacycle, P(a)—adsorbed product (either EO or Ac), and P(g)—product in the gas-phase. (For interpretation of the references to color in this figure legend, the reader is referred to the web version of this article.)

whereas the barrier for C–H bond-breaking (1.52 eV) is larger than that on Cu(100), consistent with the finding that the barrier for dehydrogenation increases with the atomic coordination of the reaction site [42,43].

To gain insight into the factors that affect catalyst selectivity toward EO synthesis, we analyzed the formation of EO and Ac separately, searching for a simple quantity correlating with the activation energies, with the aim of devising an indicator for estimating the catalyst's selectivity. Torres et al. [22] recently suggested that stabilization of the EO product decreases the barrier for EO formation due to the BEP relation, according to which the activation energy correlates linearly with the enthalpy of reaction, ΔH_r: $E^* = a + b\Delta H_r$. Fig. 2 shows the BEP fit for the formation of EO and Ac, on Rh, Cu, Ag, and Au surfaces for both (100) and (111), as well as on Ag adatom on Ag(100) and on highly oxygen-covered Ag(100). These data demonstrate that the formation of Ac follows remarkably well the BEP relation, whereas the formation of EO does so to a lesser extent (with root mean squared errors [RMSEs] of 0.18 and 0.07 eV for EO and Ac formation, respectively, with largest errors of 0.32 and 0.15 eV, respectively).

Although an approximate magnitude of the activation barriers for EO and Ac formation can be determined from the BEP principle, the BEP principle alone is not sufficiently accurate to estimate the selectivity of a catalyst toward EO formation (see Fig. 5a), which at given temperature depends on the difference between the Ac and EO activation energies, $\Delta E^* = E^*_{Ac} - E^*_{EO}$.

To identify other important factors affecting catalyst selectivity toward the formation of EO with respect to Ac formation, we considered the structural features of the TSs for both reactions. Fig. 3 compares the TSs for EO and Ac formation from OMC on Ag(100), which we label as TS^{EO} and TS^{Ac}, respectively. The main difference between the two TSs is that in TS^{EO} the C–surface bond is fully broken, whereas in TS^{Ac} both the C– and O–surface bonds are only partially broken. Indeed, in EO formation, the closure of the epoxy ring is made possible by

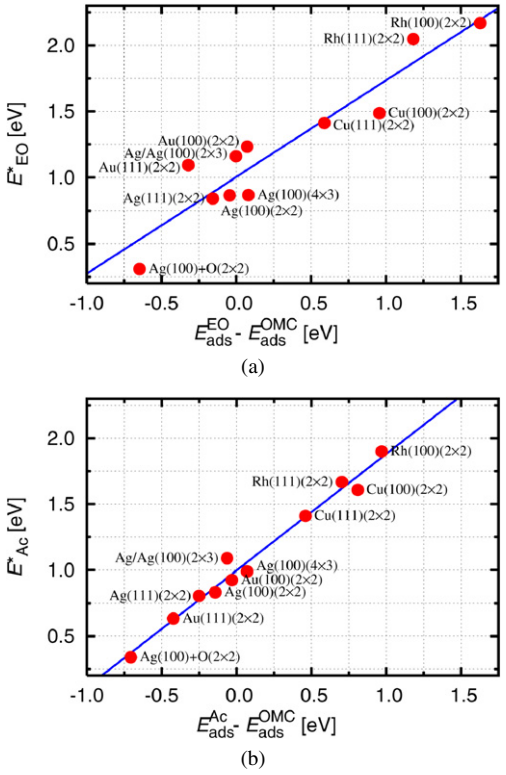

Fig. 2. Correlation between the activation energy, E^*, and the enthalpy of reaction, $\Delta H_r = E^{FS}_{ads} - E^{IS}_{ads}$, that is, Brønsted–Evans–Polanyi (BEP) relation for the formation of EO (a) and Ac (b). The RMS errors are 0.18 and 0.07 eV for (a) and (b), respectively, whereas the largest errors are 0.32 and 0.15 eV, respectively.

the oxygen shift beneath the ethylene fragment that is concomitantly lifted upward, thus breaking the C–surface bond. On the other hand, the formation of Ac involves the 1,2-hydrogen shift (i.e., the H-atom shift from the first C atom to the second) and the formation of a C=O double bond, thus breaking both the C– and O–surface bonds only partially. A comparison between the

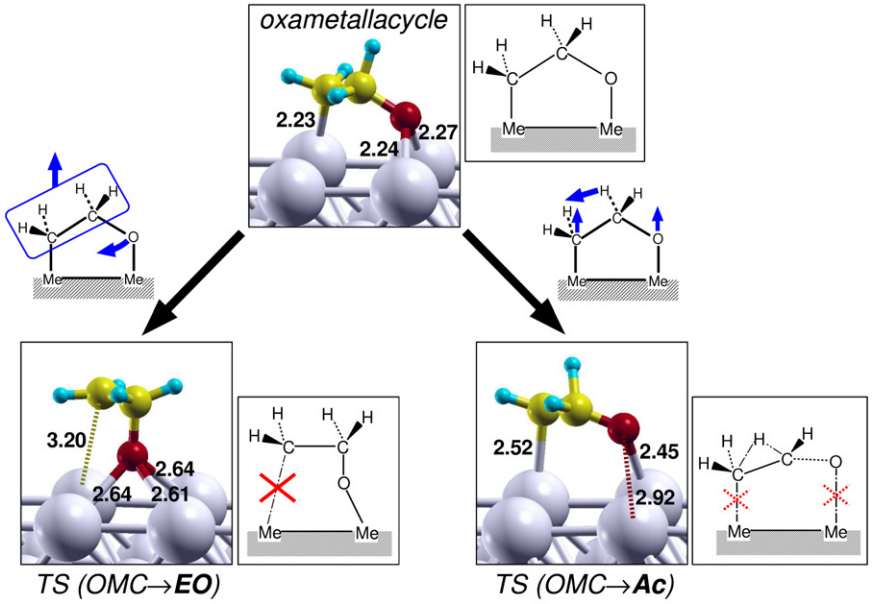

Fig. 3. Snapshots and schematic presentations of an OMC intermediate with transition states leading to EO (left) and Ac (right) on Ag(100). In the TS leading to EO the C–surface bond is broken, whereas in the TS leading to Ac both C– and O–surface bonds are elongated (distances are in Å units). During the EO formation the O-atom moves beneath the ethylene fragment, which is concomitantly shifted upward (indicated by blue arrows) and as a consequence the C–metal bond is ruptured, whereas in the formation of Ac the whole molecule is upshifted during the 1,2-hydrogen shift, and consequently the C– and O–surface bonds are partially broken.

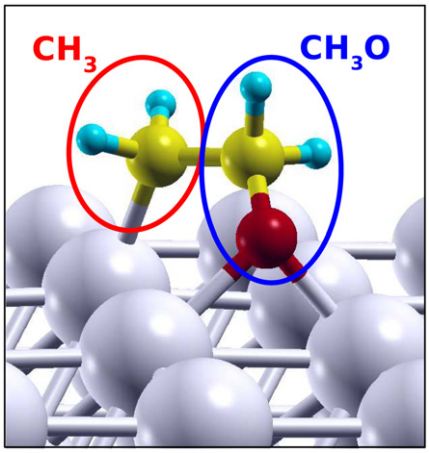

Fig. 4. The OMC–surface interaction can be decomposed into C– and O–surface terms, which can be approximated by the interaction of methyl ($CH_3\cdot$) and methoxy ($CH_3O\cdot$) radicals with the surface, respectively.

two TSs shows that the C– and O–surface bond strengths in the OMC contribute differently to the two activation energies. In particular, the stronger the OMC's O–surface bond with respect to the C–surface bond, the more selective the substrate will be toward EO formation. To make this argument more quantitative, we decompose the OMC–surface interaction into C– and O–surface contributions, which can be approximated by the interaction of methyl ($CH_3\cdot$) and methoxy ($CH_3O\cdot$) radicals with the surface, respectively, as shown in Fig. 4. We postulate that the activation energies for EO and Ac formation from OMC can be approximated as

$$E^*_{\mathrm{EO}} \simeq \alpha_1 E^{\mathrm{CH_3}}_{\mathrm{ads}} + \gamma E^{\mathrm{BEP}}_{\mathrm{EO}} + C_1,$$

and

$$E^*_{\mathrm{Ac}} \simeq \alpha_2 E^{\mathrm{CH_3}}_{\mathrm{ads}} + \beta E^{\mathrm{CH_3O}}_{\mathrm{ads}} + \gamma E^{\mathrm{BEP}}_{\mathrm{Ac}} + C_2,$$

respectively, where C_1 and C_2 are additive constants. The last term in these relations accounts for the standard BEP contribution, that is,

$$E^{\mathrm{BEP}}_{\mathrm{EO}} = E^{\mathrm{EO}}_{\mathrm{ads}} - E^{\mathrm{OMC}}_{\mathrm{ads}} \quad \text{and} \quad E^{\mathrm{BEP}}_{\mathrm{Ac}} = E^{\mathrm{Ac}}_{\mathrm{ads}} - E^{\mathrm{OMC}}_{\mathrm{ads}}.$$

The first term in E^*_{EO} accounts for the completely broken C–metal bond in $\mathrm{TS}^{\mathrm{EO}}$, whereas the first two terms in E^*_{Ac} account for the partially broken C– and O–metal bonds in $\mathrm{TS}^{\mathrm{Ac}}$. The difference between the foregoing two relations gives an approximation of the selectivity as

$$\Delta E^* \simeq \alpha E^{\mathrm{CH_3}}_{\mathrm{ads}} + \beta E^{\mathrm{CH_3O}}_{\mathrm{ads}} + \gamma\left[E^{\mathrm{Ac}}_{\mathrm{ads}} - E^{\mathrm{EO}}_{\mathrm{ads}}\right] + C,$$

where $\alpha = \alpha_2 - \alpha_1$, and C is an additive constant. A fit to the main reactions considered in this work shows that $\alpha \simeq -\beta \simeq \gamma \simeq 0.39$, as described in the Supplementary material, Section S2. We conclude that, to a very good approximation, we have

$$\Delta E^* \simeq 0.39\left[E^{\mathrm{CH_3}}_{\mathrm{ads}} - E^{\mathrm{CH_3O}}_{\mathrm{ads}} + E^{\mathrm{Ac}}_{\mathrm{ads}} - E^{\mathrm{EO}}_{\mathrm{ads}}\right] - 0.31. \qquad (1)$$

Fig. 5 compares the quality of the fit given by Eq. (1) with that obtained from the simple BEP relation. Our indicator is able to estimate ΔE^* with an accuracy better than 0.1 eV (with RMSE and maximum error of 0.05 and 0.07 eV, respectively), and it demonstrates that ΔE^* is determined mainly by two contributions: (1) the difference between the adsorption energies of CH_3 and CH_3O and (2) the difference between the adsorption energies of the two final states, Ac and EO.

Recently, Torres et al. [20] explained the larger selectivity (i.e., more positive ΔE^*) of Cu compared with Ag in terms of

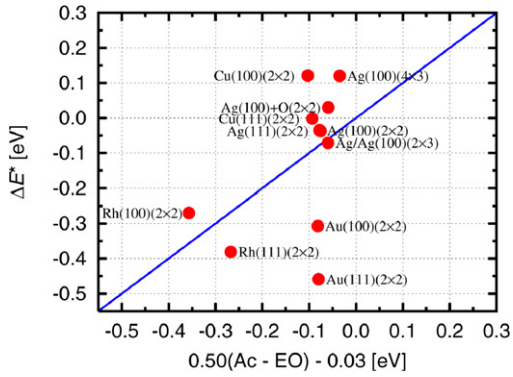

(a)

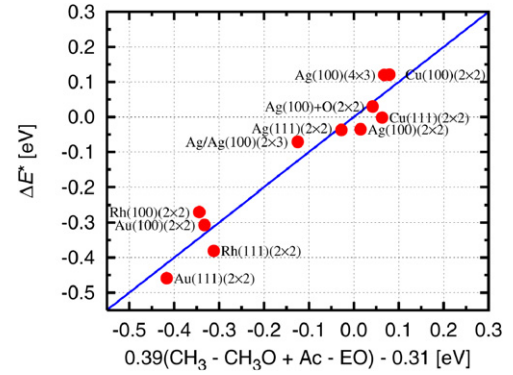

(b)

Fig. 5. Comparison of the BEP relation and Eq. (1) in predicting the $\Delta E^* = E^*_{\mathrm{Ac}} - E^*_{\mathrm{EO}}$. (a) The BEP estimation of ΔE^*: $\Delta E^* \propto E^{\mathrm{Ac}}_{\mathrm{ads}} - E^{\mathrm{EO}}_{\mathrm{ads}}$. The RMS and the maximum errors are 0.19 and 0.38 eV, respectively. (b) Fit of ΔE^* by Eq. (1). The RMS and the maximum errors are 0.05 and 0.07 eV, respectively.

different character of the $\mathrm{TS}^{\mathrm{EO}}$ of early type on Ag and late type on Cu. This observation led them to suggest that the stronger is the OMC–surface interaction, the more favored the EO formation would be with respect to the Ac. Our calculations on Rh(100) are at variance with this suggestion; the OMC–surface interaction on Rh(100) is stronger than on Cu(100), yet ΔE^* is −0.27 eV on Rh(100), lower than its value on Cu(100) of 0.12 eV. Our analysis shows instead that Cu has higher selectivity toward EO formation than the other IB metals, because Cu displays the highest relative O– vs. C–surface bond strength in OMC (first contribution in Eq. (1)). In particular, moving from Ag(100)-(2 × 2) to Cu(100)-(2 × 2) the $E^{\mathrm{Ac}}_{\mathrm{ads}} - E^{\mathrm{EO}}_{\mathrm{ads}}$ contribution to ΔE^* decreases from −0.10 to −0.15 eV, whereas the $E^{\mathrm{CH_3}}_{\mathrm{ads}} - E^{\mathrm{CH_3O}}_{\mathrm{ads}}$ increases from 0.94 to 1.16 eV.

Our model for selectivity toward EO can be easily extended to alloys. Recently, Linic et al. [17] showed on the basis of DFT calculations that Cu/Ag alloy should display a greater selectivity toward EO compared with pure Ag, a finding that was later confirmed by experiments [44,45]. However, no explanation has been given as to why this is so. Our analysis can explain this result. Cu is more reactive than Ag, and, as stated in the preceding paragraph, copper also shows greater affinity toward the O atom with respect to the C atom than silver. On diluted $\mathrm{Ag}_{1-x}\mathrm{Cu}_x$ alloys (assuming no Cu–Cu nearest neighbors), the most stable OMC binds its O atom to Cu and the C atom to Ag (e.g., such OMC orientation is preferred by 0.16 eV on Cu/Ag(100)), enhancing the O–metal bond strength and making the C–metal bond relatively weaker. According to first part of Eq. (1) (i.e., the difference between the adsorption energies of CH_3 and CH_3O), this makes the formation of EO more selective. In particular, ΔE^* is 0.17 eV higher on Cu/Ag(100) alloy than on Ag, with 0.04 eV of this due to the BEP contribution and 0.10 eV due to the C– vs. O–surface bond contribution.

4. Conclusion

In summary, for ethylene epoxidation to occur, the catalyst must be sufficiently mild so as to form an OMC rather than to break C–H bonds in either ethylene or OMC. Careful analysis of the results of DFT computer simulations allows us to disentangle two mechanisms that determine the selectivity of specific (model) catalysts at the nanometric scale. We propose a simple indicator for catalyst selectivity toward EO, as embodied by Eq. (1). In particular, for OMC to transform to EO rather than to Ac, (1) its C–metal bond has to be sufficiently weak with respect to its O–metal bond, and (2) the adsorbed EO should be stabilized against the adsorbed Ac. Thus, catalyst selectivity is determined in part by a peculiar electronic effect, which is related to the differential bonding affinity of a catalyst toward the C and O atoms of the OMC. Although the catalyst is not a perfect low-Miller index Ag surface under industrial conditions, we believe that the selectivity arguments presented here are important even under realistic conditions. More generally, we believe that the differential bonding affinity of a catalyst toward the various atoms of the molecule to which it binds may play an important role in determining selectivity in other reactions as well.

Supplementary material

The online version of this article contains additional supplementary material.

Please visit DOI: 10.1016/j.jcat.2008.01.008.

References

[1] R.A. van Santen, in: Handbook of Heterogeneous Catalysis, vol. 5, Wiley–VCH, Weinheim, Germany, 1997, p. 2244, chap. 4.6.1.
[2] J.G. Serafin, A.C. Liu, S.R. Seyedmonir, J. Mol. Catal. A 131 (1998) 157.
[3] R.M. Lambert, F.J. Williams, R.L. Cropley, A. Palermo, J. Mol. Catal. A 228 (2005) 27.
[4] M.A. Barteau, Surf. Sci. 600 (2006) 5021.
[5] J.W. Medlin, M.A. Barteau, J.M. Vohs, J. Mol. Catal. A 163 (2000) 129.
[6] J.W. Medlin, M.A. Barteau, J. Phys. Chem. B 105 (2001) 10054.
[7] S. Linic, M.A. Barteau, J. Catal. 214 (2003) 200.
[8] S. Linic, M.A. Barteau, J. Am. Chem. Soc. 124 (2002) 310.
[9] S. Linic, M.A. Barteau, J. Am. Chem. Soc. 125 (2003) 4034.
[10] S. Linic, H. Piao, K. Adib, M.A. Barteau, Angew. Chem. Int. Ed. 43 (2004) 2918.
[11] A. Klust, R.J. Madix, Surf. Sci. 600 (2006) 2025.
[12] C. Stegelmann, N.C. Schiødt, C.T. Campbell, P. Stoltze, J. Catal. 221 (2004) 630.
[13] R.L. Brainard, R.J. Madix, J. Am. Chem. Soc. 111 (1989) 3826.
[14] G.S. Jones, M. Mavrikakis, M.A. Barteau, J.M. Vohs, J. Am. Chem. Soc. 120 (1998) 2196.
[15] D. Stacchiola, G. Wu, M. Kaltchev, W. Tysoe, Surf. Sci. 463 (2000) 81.

[16] M.L. Bocquet, A. Michaelides, D. Loffreda, P. Sautet, A. Alavi, D.A. King, J. Am. Chem. Soc. 125 (2003) 5620.
[17] S. Linic, J. Jankowiak, M.A. Barteau, J. Catal. 224 (2004) 489.
[18] S. Linic, M.A. Barteau, J. Am. Chem. Soc. 126 (2004) 8086.
[19] M.-L. Bocquet, D. Loffreda, J. Am. Chem. Soc. 127 (2005) 17207.
[20] D. Torres, N. Lopez, F. Illas, R.M. Lambert, J. Am. Chem. Soc. 127 (2005) 10774.
[21] D. Torres, F. Illas, J. Phys. Chem. B 110 (2006) 13310.
[22] D. Torres, N. Lopez, F. Illas, J. Catal. 243 (2006) 404.
[23] W.-X. Li, C. Stampfl, M. Scheffler, Phys. Rev. Lett. 90 (2003) 256102.
[24] J. Schnadt, A. Michaelides, J. Knudsen, R.T. Vang, K. Reuter, E. Laegsgaard, M. Scheffler, F. Besenbacher, Phys. Rev. Lett. 96 (2006) 146101, http://link.aps.org/abstract/PRL/v96/e146101.
[25] M. Schmid, A. Reicho, A. Stierle, I. Costina, J. Klikovits, P. Kostelnik, O. Dubay, G. Kresse, J. Gustafson, E. Lundgren, J.N. Andersen, H. Dosch, P. Varga, Phys. Rev. Lett. 96 (2006) 146102, http://link.aps.org/abstract/PRL/v96/e146102.
[26] G. Henkelman, B.P. Uberuaga, H. Jonsson, J. Chem. Phys. 113 (2000) 9901.
[27] J.P. Perdew, K. Burke, M. Ernzerhof, Phys. Rev. Lett. 77 (18) (1996) 3865.
[28] S. Baroni, A. Dal Corso, S. de Gironcoli, P. Giannozzi, PWscf and phonon: Plane-wave pseudo-potential codes, 2005; http://www.pwscf.org/.
[29] S. Baroni, A. Dal Corso, S. de Gironcoli, P. Giannozzi, C. Cavazzoni, G. Ballabio, S. Scandolo, G. Chiarotti, P. Focher, A. Pasquarello, K. Laasonen, A. Trave, R. Car, N. Marzari, A. Kokalj, Quantum espresso: open-source package for research in electronic structure, simulation, and optimization, 2005; http://www.quantum-espresso.org/.
[30] D. Vanderbilt, Phys. Rev. B 41 (1990) 7892.
[31] Ultrasoft pseudopotentials for H, C, Rh, Cu, Ag, Au were taken from the PWscf PseudoPotential Download Page: http://www.pwscf.org/pseudo.htm (files: `H. pbe-rrkjus.UPF`, `C. pbe-rrkjus.UPF`, `Rh.pbe-nd-rrkjus.UPF`, `Cu.pbe-d-rrkjus.UPF`, `Ag.pbe-d-rrkjus.UPF`, and `Au.pbe-nd-van.UPF`). For the oxygen atom, the ultrasoft pseudopotential is from Ref. [46].
[32] A. Kokalj, Comput. Mater. Sci. 28 (2003) 155, code available from: http://www.xcrysden.org/.
[33] R.B. Grant, R.M. Lambert, J. Catal. 92 (1985) 364.
[34] N.F. Brown, M.A. Barteau, Surf. Sci. 298 (1993) 6.
[35] M. Mavrikakis, M.A. Barteau, J. Mol. Catal. A 131 (1998) 135.
[36] T. Hayashi, K. Tanaka, M. Haruta, J. Catal. 178 (1998) 566.
[37] R.L. Cropley, F.J. Williams, A.J. Urquhart, O.P.H. Vaughan, M.S. Tikhov, R.M. Lambert, J. Am. Chem. Soc. 127 (2005) 6069.
[38] S. Rojluechai, S. Chavadej, J.W. Schwank, V. Meeyoo, J. Chem. Eng. Jpn. 39 (2006) 321.
[39] N. Takeuchi, C.T. Chan, K.M. Ho, Phys. Rev. B 43 (1991) 14363.
[40] J.J. Cowell, A.K. Santra, R. Lindsay, R.M. Lambert, A. Baraldi, A. Goldoni, Surf. Sci. 437 (1999) 1.
[41] A.K. Santra, J.J. Cowell, R.M. Lambert, Catal. Lett. 67 (2000) 87.
[42] A. Kokalj, N. Bonini, C. Sbraccia, S. de Gironcoli, S. Baroni, J. Am. Chem. Soc. 126 (2004) 16732.
[43] A. Kokalj, N. Bonini, S. de Gironcoli, C. Sbraccia, G. Fratesi, S. Baroni, J. Am. Chem. Soc. 128 (2006) 12448.
[44] J.T. Jankowiak, M.A. Barteau, J. Catal. 236 (2005) 366.
[45] J.T. Jankowiak, M.A. Barteau, J. Catal. 236 (2005) 379.
[46] A. Dal Corso, Phys. Rev. B 64 (2001) 235118.